Distribution Network Topology Detection with Time Series Measurement Data Analysis

Guido Cavraro, Reza Arghandeh, Alexandra von Meier

***Abstract*—This paper proposes a novel approach for detecting the topology of distribution networks based on the analysis of time series measurements. The time-based analysis approach draws on data from high-precision phasor measurement units (PMUs or synchrophasors) for distribution systems. A key fact is that time-series data taken from a dynamic system show specific patterns regarding state transitions such as opening or closing switches, as a kind of signature from each topology change. The proposed algorithm here is based on the comparison of the actual signature of a recent state transition against a library of signatures derived from topology simulations. The IEEE 33-bus model is used for initial algorithm validation.**

I. Introduction

Different tools have been developed and implemented to monitor distribution network behavior with more detailed and temporal information, such as SCADA, smart meters and line sensors. Creating observability out of disjointed data streams still remains a challenge, though. Given the present monitoring technologies, more, better and faster data from behind the substation will be needed to realize smart distribution networks [1]. The cost of monitoring systems in distribution networks remains a barrier to equip all nodes with measurement devices. To some extent, a capable Distribution System State Estimation can compensate for the lack of direct sensor data to support observability. However, switches status errors can easily be misinterpreted as analog measurement errors (e.g. voltage or current readings). Thus topology detection is an important enabling component for state estimation as well as a host of other operation and control functions based on knowledge of the system operating states in real-time.

Topology detection in distribution networks is not a trivial problem. Firstly, switches may not reliably communicate their status to the distribution operator, so the topology can only be determined by sending crews into the field. Moreover, the reported switch status may be faulty due to switch malfunction and unreported maintenance crew manipulation. Integration of distributed energy resources, electric vehicles and controllable loads add more dynamics to the distribution networks that may lead to more frequent protection and switching actions. A survey of utilities experts done by the authors shows on average 5 to 10 switching actions happens under an urban distribution substation [2]. Furthermore, knowledge of the correct, updated topology is essential for safety and service restoration after outages[3].

G. Cavraro is with the Department of Information Engineering, University of Padova, Italy. Email: cavraro@dei.unipd.it.

R. Arghandeh is with the California Institute for Energy and Environment (CIEE), University of California, Berkeley, CA, USA. Email: arghandeh@berkeley.edu

Most of literature on topology detection are based on state estimator results and measurement matching with different topologies. In [4] authors propose a state estimation algorithm that incorporates switching device status as additional state variables. A normalized residual test is used to identify the best estimate of the topology. State estimation based algorithms are limited to state estimator accuracy. They are also sensitive to measurement device placement. In [5], the authors provide a tool for choosing sensor placement for topology detection. Given a particular placement of sensors, the tool reveals the confidence level at which the status of switching devices can be detected. Authors in [6] and [7] are focused on estimating the impedance at the feeder level. However, even a perfect identification of network impedance cannot always guarantee the correct topology, since multiple topologies could present very similar impedances.

The work in [8] used power flow analysis for matching substation loading and aggregated household meter load data from network connectivity modeling. They assumed metering load data are time synchronized with a measurement device on each transformer. The assumption is still far from an actual load metering system. Moreover, convergence of the proposed optimization is sensitive to bad data. Voltage measurement cross correlation for house meters data is presented in [9]. However, residential meters do not usually provide voltage measurements for utility operations. Voltage correlation-based methods in balanced feeders, feeders with PV resources, and feeders with inaccurate GIS models can be error prone. Moreover, voltage measurement in meters are hourly or 15 minute average values. Voltage average values introduce additional errors in voltage regression-based methods for topology detection. Most of the proposed methods in literature are post-processing methods which depend on correct execution of state estimation or power flow.

In this paper, a novel approach for topology detection is proposed based on time series analysis of phasor measurement unit (PMU) data. This approach is inspired by high-precision phasor measurement units for distribution systems micro-synchrophasors (μ-PMU), which the authors are involved in implementing [10]. The main idea derives from the fact that time-series data from a dynamic system show specific patterns regarding system state transitions, a kind of signature left from each topology change. The algorithm is based on the comparison of the trend vector, built from system observations, with a library of signatures derived from the possible topologies transitions. The topology detection results are impacted by load uncertainty and measurement device accuracy. Therefore, the conduced analysis takes load dynamics and measurement error into account. A set of actual secondly load measurements are used for a number of residential customers in the United States.

The derived statistical load model is applied to the topology detection scenarios to validate the proposed algorithm. The topology detection accuracy is also dependent on μ-PMU placement. We proposed a μ-PMU placement approach for topology detection application. The analysis shows that the topology detection algorithm converges even with limited measurement devices.

II. Distribution Grid Model

This section presents the distribution network model and its related notations. Given a matrix W, we denote its transpose by W^T and its conjugate transpose by W^*. We denote the matrices of the real and of the imaginary part of W by $\Re(W)$ and by $\Im(W)$, respectively. We denote the entry of W that belongs to the j-th row and to the k-th column by W_{jk}.

Given a vector v, v_j will denote its j-th entry, while v_{-j} the subvector of v, in which the j-th entry has been eliminated. We denote its complex conjugate by $\overline{v}$. Given two vectors v and w, we denote by $\langle v, w\rangle$ their inner product v^*w. We define the column vector of all ones by $\mathbf{1}$.

We associate with the electric grid the directed graph $\mathcal{G} = (\mathcal{V}, \mathcal{E})$ and the sets $\mathcal{S}$ and $\mathcal{P}$, where

- $\mathcal{V}$ is the set of nodes (the buses), with cardinality n;
- $\mathcal{E}$ is the set of edges (the electrical lines connecting the buses), with cardinality w;
- $\mathcal{S}$ is the set of switches (or breakers) deployed in the electrical grid, with cardinality r
- $\mathcal{P}$ is the set of nodes endowed with voltage phasor measurement units (PMUs), with cardinality p

Let $A \in \{0, \pm 1\}^{w\times n}$ be the incidence matrix of the graph $\mathcal{G}$,

$$A = \begin{bmatrix} a_1^T & \dots & a_w^T \end{bmatrix}^T$$

where a_j is the j-th row of A. The elements of A are all zeroes except for the entries associated with the nodes connected by the j-th edge, for which they are equal to $+1$ or -1 respectively. In this study, we consider the steady state behavior of the system, when all voltages and currents are sinusoidal signals waving at the same frequency ω_0. Thus, they can be expressed via a complex number whose magnitude corresponds to the signal root-mean-square value, and whose phase corresponds to the phase of the signal with respect to an arbitrary global reference. Therefore, x represents the signal $x(t) = |x|\sqrt{2}\sin(\omega_0 t + \angle x)$. The system state is described by the following quantities:

- $u \in \mathbb{C}^n$, where u_v is the grid voltage at node v;
- $i \in \mathbb{C}^n$, where i_v is the current injected at node v;
- $s = p + iq \in \mathbb{C}^n$, where s_v, p_v and q_v are the complex, the active and the reactive power injected at node v, respectively;
- $\sigma \in \{0, 1\}^r$, where σ_v is the staus of the breaker v: $\sigma_v = 0$ if the switch v is open, $\sigma_v = 1$ if the switch v is closed;
- $y \in \mathbb{C}^p$, where y_v is the grid voltage measured by the sensor v
- the *trend vector* $\delta(t_1, t_2) \in \mathbb{C}^p$, defined as the difference between phasorial voltages taken at the two time istant t_1 and t_2. i.e. $\delta(t_1, t_2) = u(t_1) - u(t_2)$.

We assume that the PMUs deployed in the grid take measurements at the frequency f. We denote with $\boldsymbol{T}_\sigma$ the unique topology whose switches status is described by σ. Its bus admittance matrix $\boldsymbol{Y}_\sigma$ is defined as

$$(\boldsymbol{Y}_\sigma)_{jk} = \begin{cases} \sum_{j\neq k} Y_{jk}, \text{ if } j = k \\ -Y_{jk}, \text{ otherwise} \end{cases} \tag{1}$$

where Y_{jk} is the admittance of the branch connecting bus j and bus k and where we neglect the shunt admittances. From (1), it can be seen that $\boldsymbol{Y}_\sigma$ is symmetric and satisfies

$$\boldsymbol{Y}_\sigma \mathbf{1} = 0, \tag{2}$$

i.e. $\mathbf{1}$ belongs to the Kernel of $\boldsymbol{Y}_\sigma$. Furthermore, it can be shown that if $\mathcal{G}$, the graph associated to the electrical grid, is connected, then the kernel of $\boldsymbol{Y}_\sigma$ has dimension 1.

We model the substation as an ideal sinusoidal voltage source (*slack bus*) at the distribution network nominal voltage U_N. We assume, without loss of generality, that U_N is a real number. We model all nodes but the substation as *constant power devices*, or *P-Q buses*. In the following, u_1, s_1, p_1, q_1 will denote the voltage of the substation, and its complex, its active and its reactive power injected, respectively. The system state satisfies the following equations

$$i = \boldsymbol{Y}_\sigma u \tag{3}$$

$$u_1 = U_N \tag{4}$$

$$u_v \bar{i}_v = p_v + iq_v \qquad v \neq 0 \tag{5}$$

The following Lemma [11] introduces a particular, very useful pseudo inverse of $\boldsymbol{Y}_\sigma$.

Lemma 1: There exists a unique symmetric, positive semidefinite matrix $\boldsymbol{X}_\sigma \in \mathbb{C}^{n\times n}$ such that

$$\begin{cases} \boldsymbol{X}_\sigma \boldsymbol{Y}_\sigma = I - \mathbf{1}e_1^T \\ \boldsymbol{X}_\sigma e_1 = 0. \end{cases} \tag{6}$$

Applying Lemma 1, from (3) and (4) we can express the voltages as a function of the currents and of the nominal voltage U_N:

$$u = \boldsymbol{X}_\sigma i + \mathbf{1}U_N \tag{7}$$

The following proposition ([11]) provides an approximation of the relationship between voltages and powers.

Proposition 1: Consider the physical model described by the set of nonlinear equations (3), (4), (5) and (7). Node voltages then satisfy

$$u = U_N\mathbf{1} + \frac{1}{U_N}\boldsymbol{X}_\sigma \bar{s} + o\left(\frac{1}{U_N}\right) \tag{8}$$

(the little-o notation means that $\lim_{U_N\to\infty} \frac{o(f(U_N))}{f(U_N)} = 0$). Equation (8) is derived basically from a first order Taylor expansion w.r.t. the nominal voltage U_N of the relation among powers and voltages. Even if the solutions of (8) could be not very precise, and then its application to the power flow computation could be not satisfactory, it has been already used with success in state estimation [12], Volt/Var optimization [13], and the optimal power flow problem [14].

III. Identification of Switching Actions

The basic idea behind our proposed approach is that changes of the breakers status will create specific signatures in the grid voltages. In order to develop the theoretical base for the proposed algorithm, we make the following assumptions.

Assumption 1: We assume that all the lines have the same resistance over reactance ratio. Therefore, $\Im(Y_{jk}) = \alpha\Re(Y_{jk}), \forall\, Y_{jk}$.

Assumption 2: We assume that only one switch can change its status at each time.

Assumption 3: We assume that the graph associated with the grid is always connected, i.e. that there are no admissible state in which any portion of the grid remains disconnected.

Assumption 1 will be relaxed in Section VIII, in order to test the algorithm in a more realistic scenario. However, it allows us to write the bus admittance matrix in a simpler way. In fact, due also to $\boldsymbol{Y}_\sigma$ symmetry, we can write

$$\boldsymbol{Y}_\sigma = \Re(\boldsymbol{Y}_\sigma) + i\Im(\boldsymbol{Y}_\sigma) = (1+i\alpha)U\Sigma_R U^* \tag{9}$$

where Σ_R is a diagonal matrix whose diagonal entries are the non-zero eigenvalues of $\Re(\boldsymbol{Y}_\sigma)$, and U is an orthonormal matrix that includes all the associated eigenvector. From (2), it can be shown that U spans the image of $I - \mathbf{1}\mathbf{1}^T/(\mathbf{1}^T\mathbf{1})$, i.e. the space orthogonal to $\mathbf{1}$. The matrix $\boldsymbol{X}_\sigma$ can be written as

$$\boldsymbol{X}_\sigma = (1+i\alpha)^{-1}\Lambda U\Sigma_R^{-1}U^*\Lambda^T \tag{10}$$

with $\Lambda = (I - \mathbf{1}e_1^T)$. Assumption 2 is instead reasonable for the proposed algorithm framework: it works in the scale of some seconds, while typically the switches are electro-mechanical devices and their actions are not simultaneous. Finally, Assumption 3 is always satisfied during the normal operation. We introduce the main idea that underlies our algorithm with the following example.

Example 1: Assume that at time $t-1$ the switches status is described by $\sigma(t-1) = \sigma_1$, resulting in the topology $\boldsymbol{T}_{\sigma_1}$ with bus admittance matrix $\boldsymbol{Y}_{\sigma_1}$. Applying Proposition 1 and neglecting the infinitesimal term, we can express the voltages as

$$u(t-1) = \boldsymbol{X}_{\sigma_1}\frac{\bar{s}}{U_N} + \mathbf{1}U_N \tag{11}$$

At time t the ℓ-th switch, that was previously open, changes its status. Let the new status be described by $\sigma(t) = \sigma_2$, associated with the topology $\boldsymbol{T}_{\sigma_2}$. Since we are basically adding to the graph representing the grid the edge on which switch ℓ is placed, we can write

$$\boldsymbol{Y}_{\sigma_2} = \boldsymbol{Y}_{\sigma_1} + Y_\ell a_\ell a_\ell^T \tag{12}$$

where Y_ℓ is the admittance of the line, and the elements of a_ℓ is the ℓ-th row of the adjacency matrix associated with $\boldsymbol{T}_{\sigma_2}$. Since a_ℓ is orthogonal to $\mathbf{1}$, there exists b_ℓ such that $Ub_\ell = a_\ell$. This allow us to write

$$\begin{aligned}\boldsymbol{Y}_{\sigma_2} &= (1+i\alpha)U(\Sigma_R + \Re(Y_\ell)b_\ell b_\ell^T)U^* \\ \boldsymbol{X}_{\sigma_2} &= (1+i\alpha)^{-1}\Lambda U(\Sigma_R + \Re(Y_\ell)b_\ell b_\ell^T)^{-1}U^*\Lambda^T\end{aligned} \tag{13}$$

The voltages are

$$u(t) = \boldsymbol{X}_{\sigma_2}\frac{\bar{s}}{U_N} + \mathbf{1}U_N \tag{14}$$

The trend vector $\delta(t, t-1)$ can thus be written as

$$\delta(t,t-1) = (\boldsymbol{X}_{\sigma_2} - \boldsymbol{X}_{\sigma_1})\frac{\bar{s}}{U_N} \tag{15}$$

Example 2: Consider now the opposite situation: at time $t-1$ the ℓ-th switch is closed and it is opened at time t, i.e. $\sigma(t-1) = \sigma_2, \sigma(t) = \sigma_1$. In this case we have that

$$\delta(t,t-1) = (\boldsymbol{X}_{\sigma_1} - \boldsymbol{X}_{\sigma_2})\frac{\bar{s}}{U_N} \tag{16}$$

We can observe that when there is a switching action, the voltage profile varies in a way determined by the particular transition from a topology to another. Furthermore, opening or closing a determined breaker makes the system vary in the opposite way, e.g. compare (15) with (16). This is basically due to the fact that $[\sigma_1]_{-\ell} = [\sigma_2]_{-\ell}$.

Given a breaker status σ associated with the topology $\boldsymbol{Y}_\sigma = (1+i\alpha)U\Sigma_R U^*$, and fixed an edge ℓ endowed with a breaker, associated with the row a_ℓ in the incidence matrix, we define the *signature matrix* $\Phi_{\sigma_{-\ell}}$ as

$$\Phi_{\sigma_{-\ell}} = U\Sigma_R^{-1}U^* - U(\Sigma_R + \Re(Y_\ell)b_\ell b_\ell^T)^{-1}U^* \tag{17}$$

Exploiting the signature matrix we can write

$$\delta(t,t-1) = \Lambda\Phi_{\sigma(t)_{-\ell}}\Lambda^T\frac{\bar{s}}{U_N} \tag{18}$$

if the switch ℓ has been closed, else

$$\delta(t,t-1) = -\Lambda\Phi_{\sigma(t)_{-\ell}}\Lambda^T\frac{\bar{s}}{U_N} \tag{19}$$

if the switch ℓ has been opened. The following Proposition show a characteristic of the signature matrix that is fundamental for the development of our topology detection algorithm.

Proposition 2: For every transition from the state described by $\sigma(t-1)$ to the one described by $\sigma(t)$, due to a action of the switch ℓ, $\Phi_{\sigma(t)_{-\ell}}$ is a rank one matrix.

Proof: Following the same reasoning of Example 1, and exploiting K. Miller Lemma ([15]), after some simple computations we can write

$$\Phi_{\sigma(t)_{-\ell}} = \mu U\Sigma_R^{-1}b_\ell b_\ell^T\Sigma_R^{-1}U^* \tag{20}$$

with

$$\mu = \frac{1}{1 + \mathrm{Tr}(\Re(Y_\ell)b_\ell b_\ell^T\Sigma_R)}$$

It's trivial to see that $\Phi_{w(t)_{-\ell}}$ is a rank one matrix with eigenvector

$$\hat{g}_{\sigma(t)_{-\ell}} = U\Sigma_R^{-1}b_\ell \tag{21}$$

associated with the non-zero eigenvalue

$$\lambda_{\sigma(t)_{-\ell}} = \mu\|U\Sigma_R^{-1}b_\ell\|^2 \tag{22}$$

Thus, we have

$$\Phi_{\sigma(t)_{-\ell}} = \lambda_{\sigma(t)_{-\ell}}\hat{g}_{\sigma(t)_{-\ell}}\hat{g}^*_{\sigma(t)_{-\ell}}$$

■

The trend vector $\delta(t, t-1)$ represents how the opening or the closure of a switch spreads on the voltages profile. Thanks to Proposition 2 we can write it as

$$\delta(t,t-1) == \left[\lambda_{\sigma(t)_{-\ell}} \hat{g}^*_{\sigma(t)_{-\ell}} \Lambda^T \frac{\bar{s}}{U_N}\right] \Lambda \hat{g}_{\sigma(t)_{-\ell}} \tag{23}$$

from which we see that $\delta(t, t-1) \propto \Lambda \hat{g}_{\sigma(t)_{-\ell}}$, i.e., every pattern that appears on the voltage profile due to switching actions is proportional to $\Lambda \hat{g}_{\sigma(t)_{-\ell}}$, irrespective of other variables such as voltages u and loads s that describe the network operating state at the time. Thus, $g_{\sigma(t)_{-\ell}}$ can be seen as the *particular signature* of the switch action. This fact is the cornerstone for the topology detection algorithm in this paper.

Remark 1: The opening and the closure of the switch ℓ, once the other switches status is fixed, share the same signature $g_{\sigma(t)_{-\ell}}$, thus in principle they are indistinguishable. Without any other information, the trend vector can just identify witch switch has changed its status.

IV. Topology Detection Algorithm

If we assume the distribution network physical infrastructure known, i.e. conductor impedances and switch locations, we can build a *library* $\mathcal{L}$ in which we collect all the normalized products between Λ and the eigenvectors (21) for all possible breaker actions

$$\mathcal{L} = \left\{ g_{w_{-\ell}} : w \text{ satisfies Assumption 3} \right\} \tag{24}$$

where

$$g_{\sigma(t)_{-\ell}} = \frac{\Lambda \hat{g}_{\sigma(t)_{-\ell}}}{\|\Lambda \hat{g}_{\sigma(t)_{-\ell}}\|} \tag{25}$$

It is natural to compare at each time the trend vector $\delta(t, t-1)$ with the elements in the library to identify if and which switch changed its status. As stated in Remark 1, if we want to identify which is the current topology we need additional information, i.e. the knowledge of the topology before the transition. In that case, we could compare the trend vector with a restricted portion of the library $\mathcal{L}$, since there are only r possible transitions, each of one caused by the action of one of the r breakers. As a consequence, we can compare $\delta(t, t-1)$ with the *particular library*

$$\mathcal{L}_{\sigma(t-1)} = \{ g_{\sigma(t)_{-\ell}} : \sigma(t)_{-\ell} = \sigma(t-1)_{-\ell} \} \tag{26}$$

that is peculiar of the state $\sigma(t-1)$ before the transition. The comparison is made by projecting the normalized measurements-based trend vector $\frac{\delta(t,t-1)}{\|\delta(t,t-1)\|}$ onto the topology library $\mathcal{L}_{\sigma(t-1)}$. The projection is performed with the inner product, and it allows us to obtain for each vector in $\mathcal{L}_{\sigma(t-1)}$

$$c_{\sigma(t)_{-\ell}} = \left\| \left\langle \frac{\delta}{\|\delta\|}, g_{\sigma(t)_{-\ell}} \right\rangle \right\|. \tag{27}$$

If $c_{\sigma(t)_{-\ell}} \simeq 1$, it means that δ is spanned by $g_{\sigma(t)_{-\ell}}$ and then that the switch ℓ changed its status. Because of the approximation (8), the projection will never be exactly one. Therefore, we will use a heuristic threshold, called *min_proj*, based on our numerous simulations to select the right breaker. If the projection is greater than the threshold, the associated switch is selected and the topology change time is detected. If there is no switches action, the trend vector will be zero as all the $c_{\sigma(t)_{-\ell}}$, and the algorithm will not reveal any topology transition. Thus, the projection value is used by the algorithm to detect the change time too, differently of what proposed in [16], where we used the norm of a matrix built by measurements (the *trend matrix*). The new approach is more reliable in the realistic case. With a slight abuse of notation, we will say that the maximizer of $\mathcal{C}$, denoted by $\max \mathcal{C}$, is the switches status σ such that $[\sigma]_{-\ell} = \sigma(t)_{-\ell}$, $[\sigma]_\ell = 1$ if $\sigma(t)_{-\ell} = 0$ or vice-versa $[\sigma]_\ell = 0$ if $\sigma(t)_{-\ell} = 1$ and $c_{\sigma(t)_{-\ell}}$ its the maximum element in $\mathcal{C}$.

We tacitly assumed so far all the buses endowed with a PMU, just to show the main idea. But this is not a realistic scenario for a distribution network. Now we show how the former approach can be generalized in presence of limited information, in which we are allowed to take only a few voltage measures:

$$\begin{aligned} y &= I_{\mathcal{P}} u \\ &= I_{\mathcal{P}} \boldsymbol{X}_{\sigma(t)} \frac{\bar{s}}{U_N} + \mathbf{1} U_N \end{aligned} \tag{28}$$

where $I_{\mathcal{P}} \in [0,1]^{p \times n}$ is a matrix that select the entries of u where a PMU is placed. In that case, the trend vector becomes

$$\delta(t_1, t_2) = y(t_1) - y(t_2) \tag{29}$$

The library vectors and their dimension change too. In fact one can easily show, using (28) and retracing (14) and (20) that (25) becomes

$$g_{\sigma(t)_{-\ell}} = \frac{I_{\mathcal{P}} \Lambda \hat{g}_{\sigma(t)_{-\ell}}}{\|I_{\mathcal{P}} \Lambda \hat{g}_{\sigma(t)_{-\ell}}\|} \tag{30}$$

The topology detection algorithm with limited measurements is stated in Algorithm 1.

Algorithm 1 Topology Changes Detection

Require: At each time t, $\sigma(t-1)$, *min_proj* = 0.98

1: $\sigma(t) \leftarrow \sigma(t-1)$
2: each PMU at each node j record voltage phasor measurements $y_j(t)$
3: the algorithm builds the trend vector $\delta(t, t-1)$
4: the algorithm projects $\delta(t, t-1)$ in the library $\mathcal{L}_{\mathcal{P},\sigma(t)}$ obtaining the set of values

$$\mathcal{C} = \left\{ c_{\sigma(t)_{-\ell}} = \left\| \left\langle \frac{\delta}{\|\delta\|}, g_{\sigma(t)_{-\ell}} \right\rangle \right\|, g_{\sigma(t)_{-\ell}} \in \mathcal{L} \right\};$$

5: **if** $\max \mathcal{C} \geq$ *min_proj* **then**
6: $\quad \sigma(t) \leftarrow \arg\max \mathcal{C}$
7: **end if**

V. PMUs placement

When we have a limited number of sensors to be deployed in the distribution grid, the first requirement to be satisfied is the system *observability*, i.e. the algorithm capability of

detecting every topology transition. Since our algorithm is basically based on the comparison between trend vectors and the library vectors, the trivial condition for the observability of the network is that each vector of the library is not proportional to any of the others. The former property is equivalent to the following condition.

Lemma 2: Given the set of nodes endowed with PMUs $\mathcal{P}$, let, with a slight abuse of notation, the juxtaposition of the library vectors be denoted by $\mathcal{L}$. Let $\mathcal{L}_\mathcal{P} = I_\mathcal{P}\mathcal{L}$. Then if

$$(|\mathcal{L}_\mathcal{P}^*\mathcal{L}_\mathcal{P}|)_{uv} < 1, \forall u \neq v \tag{31}$$

the switch that changes its status can be identified.
Notice that the element $(\mathcal{L}_\mathcal{P}^*\mathcal{L}_\mathcal{P})_{uv}$ is simply the projection of $g_{[\sigma(t)]_{-u}}$ onto $g_{[\sigma(t)]_{-v}}$. If they are note purely proportional, trivially the magnitude of their inner product is smaller than one. Condition (31) can be too restrictive, if we know the switches status before the topology change. In that case, in fact, we can just check if each vector of the *particular* library is not proportional to any of the others. The former property is equivalent to the following condition.

Lemma 3: Let the switches status be σ, and let it be known. Given the set of nodes endowed with PMUs $\mathcal{P}$, let, with a slight abuse of notation, the juxtaposition of the particulary library vectors be denoted by $\mathcal{L}_\sigma$. Let $\mathcal{L}_{\mathcal{P},\sigma} = I_\mathcal{P}\mathcal{L}_\sigma$. Then if

$$(|\mathcal{L}_{\mathcal{P},\sigma}^*\mathcal{L}_{\mathcal{P},\sigma}|)_{uv} < 1, \forall u \neq v, \forall \sigma \tag{32}$$

each switch action can be identified.

Lemmas 2 and 3 can be used to infer, given the electrical grid model, which is the minimun number of PMUs to be deployed in order to have the observability.

A second issue is to find an "optimal" placement. Now we propose a simple, even if onerous, strategy for placement. After finding a minimal number of sensors and a place that guarantee the satisfaction of Lemma 2, we propose a greedy PMU placement procedure based on the sequential addition of one PMU at a time able to provide the best performance improvement, verified by Monte Carlo simulations. For every possible new place for PMU, we run num_run Monte Carlo simulation, of length TSTOP. For each of them we choose, randomly, the initial σ, the switch ℓ that changes its status and the time τ of the action. The place for the new PMU that performs the minimum number of errors is then chosen.

Algorithm 2 Greedy PMU placement

Require: $\mathcal{P}$ such that the network is observable, num_run, TSTOP
min $\leftarrow \infty$
minimizer $\leftarrow \emptyset$
for every possible place $j \notin \mathcal{P}$ **do**
  err $\leftarrow 0$
  for $t = 1$ to num_run **do**
    choose $\sigma \sim \mathcal{U}([0,1]^r)$
    choose $\ell \sim \mathcal{U}([0, \dots, r])$
    choose $\tau \sim \mathcal{U}([0, \dots, \text{TSTOP}])$
    run Monte Carlo simulations
    err = number of errors
    if err $\leq$ min **then**
      min $\leftarrow$ err
      minimizer $\leftarrow j$
    end if
  end for
end for
$\mathcal{P} \leftarrow \mathcal{P} \cup \{\text{minimizer}\}$

VI. Switching action in the non-ideal scenario

So far, we considered the case in which the measurements devices were not affected by noise and the loads were static, which is not a realistic case.

The measurement apparatus in a bus where measurements are taken is formed by a PMU and by a potential transformer (PT). A PT for metering aims to reduce the voltage magnitude, in order to make it measurable by a PMU. Both the PMU and the PT introduce errors to the voltage measured. We model the output of our PMU placed at bus j at time t by

$$y_j(t) = u_j(t) + e_j(t) + b_j(t) \tag{33}$$

where $e_j \in \mathbb{C}$ is the error introduced by the PMU, while $b_j \in \mathbb{C}$ is the errors introduced by the PT. A common characterization of the error is the *total vector error* (TVE). For example if x is the variable to be measured, and x^N is the measured value, the TVE is

$$\text{TVE} = \frac{|x - x^N|}{|x|} \tag{34}$$

Furthermore, the loads are not static but they have a natural dynamic. In this paper we assume that the loads have *constant power factor*, and consequently

$$\frac{q(t)_j}{p(t)_j} = \gamma_j, \quad \forall t,\ j = 2, \dots, n. \tag{35}$$

We model the active power and the reactive power consumption at each load by

$$p(t+1)_{-1} = p(t)_{-1} + n_p(t) \tag{36}$$

$$q(t)_{-1} = \text{diag}(\gamma_2, \dots, \gamma_n)p(t)_{-1} \tag{37}$$

where $n_p(t)$ is a Gaussian random vector. This could seems too rough and unsophisticated, but we will see in section VII that is actually enough accurate.

If we take into account (33), (36) and (37), the trend vector becomes

$$\delta(t_1, t_2) = I_\mathcal{P}(\boldsymbol{X}_{\sigma(t_1)} - \boldsymbol{X}_{\sigma(t_2)})\frac{\bar{s}(t_2)}{U_N} + e_{t_1} - e_{t_2} + \\ + b_{t_1} - b_{t_2} + \frac{I_\mathcal{P}\boldsymbol{X}_{\sigma(t_1)}}{U_N}\sum_{t=t_2}^{t_1-1} n_p(t) - in_q(t), \tag{38}$$

being $p(t_1)_{-1} = p(t_2)_{-1} + \sum_{t=t_2}^{t_1-1} n_p(t)$.Since a PT is a passive device and since in the following we will consider only fast measurement rate, we approximate satisfactorily the errors introduced by a PT with a constant, i.e. we will assume that $b_j(t) = b_j$. As a consequence, the term $b_{t_1} - b_{t_2}$ in (38) vanishes. Because of measurements noise and loads dynamic,

the trend vector is typically non-zero even if there has not been any switching action, and the projection (27) may be almost one, leading to false topology detection. When any switch is closed or opened, since we are adding or deleting a branch, we are changing the currents flows, reflecting on an abrupt, greater voltages variation. Therefore, a first strategy to avoid false positive is to not consider trend vector whose norm is lower than a defined threshold, called in the following *min_norm*. Moreover the additive noise can make the maximum projection value of the trend vector $\max \mathcal{C}$ onto the library vectors considerably lower than one, even if a topology change occurred. This fact prompts us to use a value for *min_proj* lower than the one considered in Algorithm 1. Of course, the use of a lower threshold makes the algorithm more vulnerable to false positive. The following example will give the idea for a possible solution.

Example 3: Assume the grid without load variation and measurements noise, and that at time t_1 the ℓ-th switch change its status. Consider the trend vector

$$\delta(t, t-\tau) = y(t) - y(t-\tau).$$

For $t < t_1$ and $t \geq t_1 + \tau$ the projections of the trend vector onto the library are all equal to zero, because

$$\delta(t, t-\tau) = y(t) - y(t-\tau) = 0$$

Instead for $t_1 \leq t < t_1 + \tau$, the trend vector is

$$\delta(t, t-\tau) = \Lambda \Phi_{\sigma(t)_{-\ell}} \Lambda^T \frac{\bar{s}}{U_N}$$

leading to a cluster of algorithm time instant of length τ (or $\frac{\tau}{f}$ seconds), in which the maximum projection coefficient will be almost one.

A possible solution is thus to consider a trend vector built using not two consecutive measures, but considering measures separated by τ algorithm time istants , i.e.

$$\delta(t, t-\tau) = y(t) - y(t-\tau).$$

and to assume that a topology change has happened at time t when we have a cluster whose length length_cluster is τ of consecutive values of $\max \mathcal{C}$ greater than min_proj. This idea will be clarified with some simulations in Section VIII. The former observations lead to the Algorithm 3 for topology detection with measurements noise and load variation.

Algorithm 3 Topology transition detection with noise

Require: At each time t, we are given the variables $\sigma(t-1)$, minimizer$(t-1)$, length_cluster$(t-1)$

$\sigma(t) \leftarrow \sigma(t-1)$
each PMU at each node j record voltage phasor measurements $y_j(t)$
the algorithm builds the trend vector $\delta(t, t-\tau)$
if $\|\delta(t, t-\tau)\| <$ min_norm **then**
    $\delta(t, t-\tau) \leftarrow 0$
    minimizer$(t) = 0$
    length_cluster$(t) = 0$
else
    the algorithm projects $\delta(t, t-\tau)$ in the particular library $\mathcal{L}_{\mathcal{P},\sigma(t)}$ obtaining the set of values

$$\mathcal{C} = \left\{ c_{\sigma(t)_{-\ell}} = \left\| \left\langle \frac{\delta}{\|\delta\|}, g_{\sigma(t)_{-\ell}} \right\rangle \right\|, g_{\sigma(t)_{-\ell}} \in \mathcal{L} \right\};$$

    if $\max \mathcal{C} >$min_proj **then**
        minimizer$(t) = \arg\min \mathcal{C}$
        if minimizer$(t) =$ minimizer$(t-1)$ **then**
            length_cluster$(t) \leftarrow$ length_cluster$(t-1)$ + 1
            if length_cluster$(t) = \tau$ **then**
                $\sigma(t) \leftarrow$ minimizer(t)
            end if
        else
            length_cluster$(t) \leftarrow 1$
        end if
    end if
end if

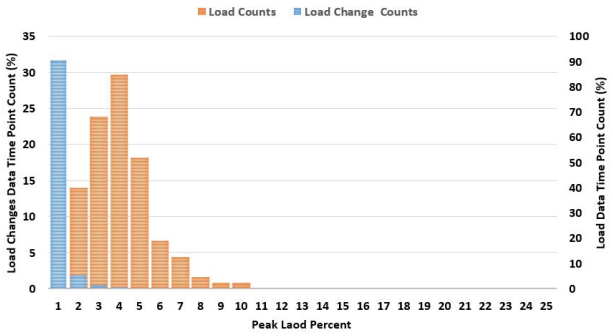

Figure 1. Load variability and load change variability based on normalized load values.

VII. Dynamic Characterization of Actual Loads

Load behavior at the individual customer level and at high time resolution can be a critical question in distribution networks. Due to lack of accurate and high resolution measurements at meters, there is no a clear answer to that question. The most commonly available data from loads come from meters with hourly (or 15 minutes) time intervals. For applications that are based on network parameters in shorter time than hourly, large uncertainty is caused by low resolution load data. For our topology detection algorithm, the load variation is very important, since it affects the topology detection capability, as (38) shows. To add more practicality to the proposed topology detection algorithm, a load measurement data set for five houses in the United States is used. Load demand (kW) is recorded every second for a week. Statistical analysis of these load data is presented in Table I. Table II reports instead the statistical analysis of the variation of the load demand between two consecutive seconds. The field "Relative SD" expresses the standard deviation of the load or of the load change as a percentage of the load peak value, written in Table I. Figure 1 shows the histogram of load duration and load changes. The orange bars represents measurements data points over the percentage of pick load values. The blue bars show load change

Table I. LOAD VALUES

	SD (kW)	Max (kW)	Relative SD (%)
House 1	0.415	5.990	6.93
House 2	1.309	10.956	11.95
House 3	1.955	11.578	16.88
House 4	2.566	12.364	20.75
House 5	1.309	8.155	16.06
Aggregate	4.204	27.229	15.44

Table II. LOAD VARIATION

	Mean (kW)	SD (kW)	Relative SD (%)
House 1	0.000	0.045	0.11
House 2	0.000	0.070	0.64
House 3	0.000	0.113	0.98
House 4	0.000	0.110	0.89
House 5	0.000	0.046	0.56
Aggregate	0.000	0.184	0.68

in one second intervals over the percentage of pick load values. In case of load changes, more than 90 percent of measurement time points have loads with less that one percents of pick load. It means that during one second time intervals, there is not huge difference in load data. In the United States, a number of houses are connected to one distribution transformer. Therefore, the aggregated five houses loads are considered as the reference for load variability in this paper. The lower the measurements frequency, the higher the load variability. Resampling the data, we obtain the aggregated characterization reported in Table III for different measurements frequencies, i.e. for one measure every second, one measure every five seconds and one measure every ten seconds. Further numerical analysis shows that the load differences, for all the frequencies, can be modeled as Gaussian random variables thus validating equations (36) and (37), that can be assumed as a realistic model of load variation.

VIII. RESULTS, DISCUSSIONS AND CONCLUSIONS

We tested our algorithm for topology detection on the IEEE 33-bus distribution test feeder [17], which is illustrated in the Figure 2. In this testbed, there are five breakers (namely S_1, S_2, S_3, S_4, S_5) that can be opened or closed, thus leading to the set of 32 possible topologies $\boldsymbol{T}_1, \ldots, \boldsymbol{T}_{32}$. Because of the ratio between the number of buses and the number of switches, some very similar topologies can occur (for example the topology where only S_1 is closed and the one in which only S_2 is closed). In the IEEE33-bus test case, Assumption 1 about line impedances does not hold, making the test condition more realistic. Each bus of the network represent an aggregate of five houses, whose power demand is described by the statistical Gaussian model derived in Section VII, dependent on the sampling frequency, and whose characterization is reported in Table III. Regarding the measurement noise, we assume that the buses are endowed with high precision devices, the μPMU [18], and with PTs. PMUs measurements are effected

Table III. LOAD VARIATION FOR DIFFERENTS FREQUENCY

	Mean (kW)	SD (kW)	Relative SD (%)
$f = 1$ Hz	0.000	0.184	0.68
$f = 0.2$ Hz	0.000	0.425	1.56
$f = 0.1$ Hz	0.000	0.604	2.22

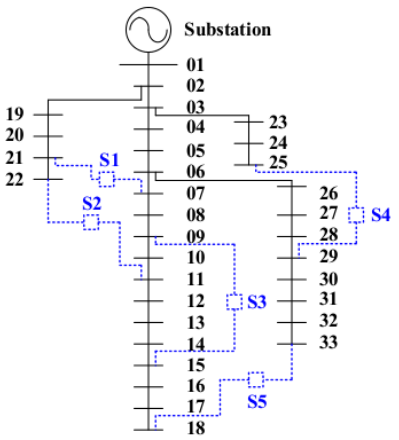

Figure 2. Schematic representation of the IEEE33 buses distribution test case with the five switches

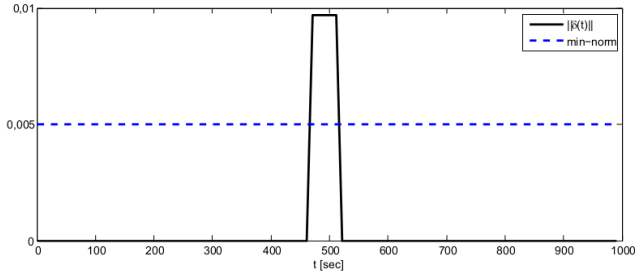

Figure 3. Trend vector norm with noiseless measurements and loads non time varying

by Gaussian noise such that TVE $\leq 0.05\%$, based on the PMU manufacturer test information. It is also comply the IEEE standard C37.118.1-2011 for PMUs [19]. The PTs instead introduce a constant error (but peculiar of each node) that satisfy the requirements of the standard [20].

A. Trend vectors and noise treatment strategy

Here we provide simulations that show the problems given by noise and that validate the strategy we use to overcome these problems. The overall time window simulated is of 1000 seconds, the measures frequency is of one every 10 seconds and the topology transition ($f = 1/10$ sec^{-1}), from $\sigma_1 = (1, 1, 1, 0, 1)$ to $\sigma_2 = (1, 1, 0, 0, 1)$, happens at $t = 480$ sec. In Figure 3 we see what happens to the trend vector norm, while in Figure 4 we plot $\max \mathcal{C}$, when we are in a noiseless scenario with loads not time varying. We can see that the switch action instant is clear. In the case with measurements noise and time varying loads, the trajectory of the trend vector norm, compared with *min_norm* numerically setted to 0.05, is reported in Figure 5. In Figure 6 instead we plot $\max \mathcal{C}$, without putting to zero the trend vectors whose norm is lower than *min_norm* before the projection. We see that there are several cluster of time istants in which $\max \mathcal{C}$ is greater than *min_norm*, and this leads to a number of faulse positive. In Figure 7 we plot $\max \mathcal{C}$, after putting to zero the trend vectors

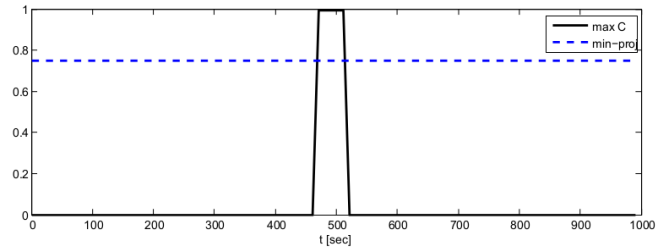

Figure 4. Trajectory of the $\max \mathcal{C}$ with noiseless measurements and loads non time varying

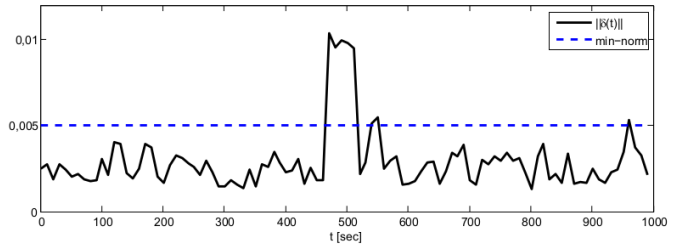

Figure 5. Trend vector norm with noisy measurements and time varying loads

whose norm is lower than *min_norm* before the projection. We still have more than one cluster, but only one has a length of $\tau\frac{1}{f}$ seconds, thus revealing the switch action instant, and the validity of our strategy.

B. Simulation of the algorithm

Here we tested the entire switches monitoring algorithm, in different situations and with different placements of PMUs:

- $\mathcal{P}_{33} = \{1, \ldots, 33\}$, where every node is endowed with a PMU;
- $\mathcal{P}_{15} = \{3, 8, 9, 10, 12, 15, 16, 17, 18, 19, 21, 24, 25, 27, 30\}$, where there are 15 PMUs, almost one every two nodes;
- $\mathcal{P}_7 = \{9, 12, 15, 18, 24, 27, 30\}$, where there are 7 PMUs, almost one every four nodes

$\mathcal{P}_{15}$ and $\mathcal{P}_7$ has been computed using Algorithm 2. The algorithm has been tested in each condition via 10000 Monte Carlo simulations.. Firstly we tested the algorithm in the ideal case without load variation nor measurement noise, resulting in no errors. Therefore, we can see that in the steady-state condition

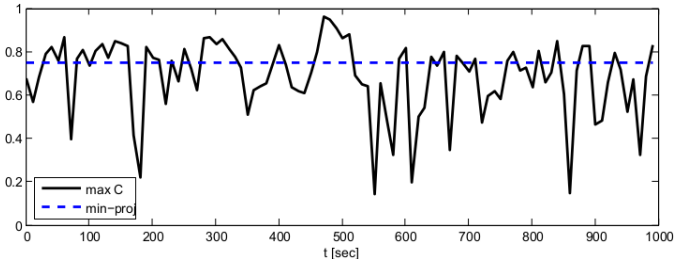

Figure 6. Trajectory of the $\max \mathcal{C}$ with noisy measurements and time varying loads

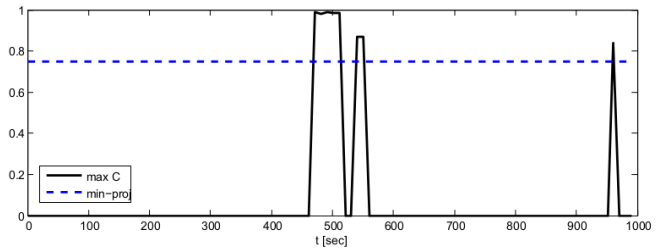

Figure 7. Trajectory of the $\max \mathcal{C}$ with noisy measurements and time varying loads after putting to zero the vectors whose norm is lower than *min_norm*

Table IV. SIMULATION RESULTS WITH 33 PMUS

SD [kV]	non detections	wrong detection	decision errors	total errors	perc. of errors (%)
0	0	50	50	100	1.00
0.68, ($f = 1$ Hz)	0	64	67	131	1.31
1.56, ($f = 0.2$ Hz)	17	131	152	300	3.00
2.22, ($f = 0.1$ Hz)	72	211	244	527	5.27

and in the absence of noise, the algorithm is extremely efficient for the 33-bus test case. It also overcomes the linearization from Proposition 1 and the initial Assumption 1. Secondly we added the measurement noise and different levels of load variation (or alternatively of measures frequency). The results are reported in Table IV, Table V and Table VI. The field "non detection" refers to the number of run in which the algorithm doesn't comprehend that there has been a switching action, the field "wrong detection" refers to the number of times the algorithm detects a false action, while "decision errors" is the number of times the algorithm provide a wrong breakers status estimation. Of course every time there is a wrong detection, we have a decision error, too. If we subtract the values of the second column to the values of the third, we find very small number, meaning that, once detected the exact action time, the algorithm works very well. The main challenge is therefore to detect the topology transition time. However our approach is very robust with the number of sensors: the percentage of errors with only 7 PMUs (where we have partial information on the grid state) is always worst than the one with 33 PMUs (where we have global information on the grid state) less than 2.5%, and probably with the best parameter tuning (*min_norm* and *min_proj*), it can still be improved.

Table V. SIMULATION RESULTS WITH 15 PMUS

Relative SD (%)	non detections	wrong detection	decision errors	total errors	perc. of errors (%)
0	0	52	52	104	1.04
0.68, ($f = 1$ Hz)	0	73	76	149	1.49
1.56, ($f = 0.2$ Hz)	29	135	158	322	3.22
2.22, ($f = 0.1$ Hz)	74	213	252	539	5.39

Table VI. SIMULATION RESULTS WITH 7 PMUS

Relative SD (%)	non detections	wrong detection	decision errors	total errors	perc. of errors (%)
0	0	56	56	112	1.12
0.68, ($f = 1$ Hz)	2	180	185	367	3.65
1.56, ($f = 0.2$ Hz)	31	199	209	441	4.41
2.22, ($f = 0.1$ Hz)	76	245	298	619	6.19

IX. Conclusions

In this paper we propose a novel strategy for the monitoring and the identification of switches action in a distribution grid. The novelty of this algorithm is the possibility of running it in real time and the fact that it could work satisfactorily with only a partial knowledge of the grid state. It allows us, exploiting a voltage phasorial measurements, to understand both the time of the switching action and the new topology, by comparing the trend vector, built by data, with other vectors contained in a library, that represent the a priori knowledge of the electrical network. The algorithm has been tested in a realistic scenario, where both measurement noise and load variation had realistic characterization. In particular, we provide a simply but plausible model of the fast time scale load variation, validated using real field load data. The simulations show the algorithm behavior in different scenario. In the ideal one, with static loads and perfect measurements devices, the algorithm gives no errors. When instead we have noisy PMUs and load variation, we still have satisfactory results, strengthened by the fact that the algorithm performance are very similar both in the case of one PMU per bus or of one PMU every four nodes.

References

[1] "Chapter 34 - every moment counts: Synchrophasors for distribution networks with variable resources," in *Renewable Energy Integration*, L. E. Jones, Ed. Boston: Academic Press, 2014, pp. 429–438.

[2] A. von Meier, M. L. Brown, R. Arghandeh, L. Mehrmanesh, L. Cibulka, and B. Russ, "Electric distribution advanced monitoring plan (amp)," in *Electric distribution Advanced Monitoring Plan*, 2014.

[3] C. Lueken, P. M. Carvalho, and J. Apt, "Distribution grid reconfiguration reduces power losses and helps integrate renewables," *Energy Policy*, vol. 48, no. 0, pp. 260 – 273, 2012, special Section: Frontiers of Sustainability. [Online]. Available: http://www.sciencedirect.com/science/article/pii/S0301421512004351

[4] G. N. Korres and N. M. Manousakis, "A state estimation algorithm for monitoring topology changes in distribution systems," in *Power and Energy Society General Meeting, 2012 IEEE*. IEEE, 2012, pp. 1–8.

[5] Y. Sharon, A. M. Annaswamy, A. L. Motto, and A. Chakraborty, "Topology identification in distribution network with limited measurements," in *Innovative Smart Grid Technologies (ISGT), 2012 IEEE PES*. IEEE, 2012, pp. 1–6.

[6] M. Ciobotaru, R. Teodorescu, and F. Blaabjerg, "On-line grid impedance estimation based on harmonic injection for grid-connected pv inverter," in *Industrial Electronics, 2007. ISIE 2007. IEEE International Symposium on*, June 2007, pp. 2437–2442.

[7] M. Liserre, F. Blaabjerg, and R. Teodorescu, "Grid impedance estimation via excitation of lcl -filter resonance," *Industry Applications, IEEE Transactions on*, vol. 43, no. 5, pp. 1401–1407, Sept 2007.

[8] V. Arya, D. Seetharam, S. Kalyanaraman, K. Dontas, C. Pavlovski, S. Hoy, and J. R. Kalagnanam, "Phase identification in smart grids," in *Smart Grid Communications (SmartGridComm), 2011 IEEE International Conference on*, Conference Proceedings, pp. 25–30.

[9] T. A. Short, "Advanced metering for phase identification, transformer identification, and secondary modeling," *Smart Grid, IEEE Transactions on*, vol. 4, no. 2, pp. 651–658, 2013.

[10] A. von Meier, D. Culler, A. McEachern, and R. Arghandeh, "Micro-synchrophasors for distribution systems," in *Innovative Smart Grid Technologies Conference (ISGT), 2014 IEEE PES*, Feb 2014.

[11] S. Bolognani and S. Zampieri, "A distributed control strategy for reactive power compensation in smart microgrids," *IEEE Trans. on Automatic Control*, vol. 58, no. 11, November 2013.

[12] L. Schenato, G. Barchi, D. Macii, R. Arghandeh, K. Poolla, and A. Von Meier, "Bayesian linear state estimation using smart meters and pmus measurements in distribution grids," in *IEEE International Conference on Smart Grid Communications 2014*. IEEE, 2014.

[13] S. Bolognani, R. Carli, G. Cavraro, and S. Zampieri, "Distributed reactive power feedback control for voltage regulation and loss minimization," 2015.

[14] G. Cavraro, R. Carli, and S. Zampieri, "A distributed control algorithm for the minimization of the power generation cost in smart micro-grid," in *Conference on Decision and Control (CDC14)*, 2014.

[15] K. S. Miller, "On the inverse of the sum of matrices," *Mathematics Magazine*, pp. 67–72, 1981.

[16] G. Cavraro, R. Arghandeh, G. Barchi, and A. von Meier, "Distribution networ topology detection with time-series measurements," in *Innovative Smart Grid Technologies (ISGT), 2015 IEEE PES*. IEEE, 2015.

[17] R. Parasher, "Load flow analysis of radial distribution network using linear data structure," *arXiv preprint arXiv:1403.4702*, 2014.

[18] "Pqube 3, new low cost, high-precision power quality, energy and environment monitoring," in *Power Standard Lab. Inc. (PSL),http://www.powerstandards.com/*.

[19] "Ieee standard for synchrophasor measurements for power systems," *IEEE Std C37.118.1-2011 (Revision of IEEE Std C37.118-2005)*, pp. 1–61, Dec 2011.

[20] I. Std, "60044-2,instrument transformers–part 2: Inductive voltage transformers," *International Electrotechnical Commission, Geneva (Switzerland)*, 1997.